

Nonclassical light generation by Coulomb blockade of resonant tunneling

A. Imamoglu and Y. Yamamoto

NTT Basic Research Laboratories, 3-9-11 Midori-cho, Musashino-shi, Tokyo 180, Japan

(Received 6 July 1992)

We show that the Coulomb blockade of resonant tunneling in semiconductor heterojunctions creates correlations between single-charge tunneling and single-photon emission events. When driven by a constant-current source, a mesoscopic *p-i-i-i-n* junction generates a regulated single-photon stream by single-electron-to-single-photon conversion. Under constant-voltage operation, the photon stream generated by the junction is antibunched and sub-Poissonian. The single-electron charging energy of the heterostructure has to exceed the width of the resonant subband and the characteristic energy of the thermal fluctuations for these correlations to be observable.

I. INTRODUCTION

There has been considerable interest in ultras-small tunnel junctions with capacitances small enough that the single-electron charging energy ($e^2/2C$) exceeds the characteristic energy (kT) of the thermal fluctuations at low temperatures.^{1,2} When such a junction is driven by a constant-current source, there will be a sequence of continuous uniform charging followed by discrete tunneling, resulting in sawtooth oscillations of the junction voltage. In the case of constant-voltage-driven two (or multi)-junction systems, the tunneling events across the two junctions are strongly correlated. This correlation results in conductance oscillations and a periodic modulation of the current-voltage characteristics. This effect in two-junction systems has been observed experimentally.³

Recently, semiconductor quantum-well and -dot structures have attracted increasing attention, as they provide a medium where both Coulomb blockade and quantum confinement effects are simultaneously important.⁴ Both theoretical⁵ and experimental⁶ efforts have been focused on the characteristics of the constant-voltage-driven double-barrier *n-i-i-i-n* resonant-tunneling structures. Possible implications of the Coulomb blockade of resonant tunneling on quantum optics have not been considered so far, since photon generation by radiative recombinations is negligible in the analyzed structures.

We have recently proposed⁷ a low-capacitance, constant-current-driven *p-p-i-n* microjunction where the Coulomb interactions regulate the electron-thermionic-emission events from the *n*-type $\text{Al}_x\text{Ga}_{1-x}\text{As}$ layer into the *p*-type GaAs layer. As a result of this regulation, the junction voltage exhibits a sawtooth oscillation pattern, with peak-to-peak amplitude e/C_{dep} and period e/I . Provided that the radiative recombination with a hole takes place in a short time scale compared to the charging time (e/I), the regulated single-electron-emission events in such a scheme are converted into regulated single-photon-emission events.⁸ Furthermore, if the microjunction is embedded in a microcavity structure⁹ where practically all the spontaneous emission goes to a single model of the radiation field, the scheme proposed in Ref. 7 generates a single-photon stream.

In this paper, we study the Coulomb-blockade-induced correlations between single-charge resonant tunneling and single-photon generation events. The basic structure that we consider is a *p-i-i-i-n* $\text{Al}_x\text{Ga}_{1-x}\text{As}$ -GaAs microjunction, where resonant tunneling of an electron and a hole into the *i*-type GaAs layer will result in photon generation by radiative recombination. The principal result of this paper is that light generated by such a microjunction is inherently nonclassical. We show that under constant-current operation, the correlation between the successive resonant-tunneling events results in regulated junction-voltage oscillations, together with the generation of a single-photon stream. Under constant-voltage operation, the photon-emission and resonant-tunneling events are strongly correlated, even though there is not strict regulation of the individual resonant-tunneling events. In both cases, the generated photons are antibunched¹⁰ and sub-Poissonian, properties that cannot be explained by conventional semiclassical theories that do not quantize the free-radiation field.

Figure 1(a) shows the generic structure of the *p-i-p-i-i-n* $\text{Al}_x\text{Ga}_{1-x}\text{As}$ -GaAs heterojunction considered in this paper. We choose the width L_i of the *i*-type GaAs layer to be 50 Å and the impurity concentrations in the *n*- and *p*-type $\text{Al}_x\text{Ga}_{1-x}\text{As}$ layers to be $n_D = 7.0 \times 10^{15}$ and $n_A = 8.0 \times 10^{16}$, respectively. For a micropost diameter of $2b = 1.0 \mu\text{m}$, the effective (undepleted) area of the junction is $A_{\text{eff}} = \pi a^2 \approx 1.8 \times 10^{-10} \text{ cm}^2$ ($2a = 0.15 \mu\text{m}$). Choosing a different Al concentration (y) in the undoped *i*-type $\text{Al}_x\text{Ga}_{1-x}\text{As}$ layer enables us to move the energy of the conduction-electron and valence-hole subbands as desired. For the assumed ionized-impurity concentrations in the *n* and *p* layers, the Fermi level is well within the conduction and valence bands, respectively. We estimate the Fermi energy in the *n* layer (E_{fn}) to be about 0.002 eV above the conduction-band minimum, and that in the *p* layer (E_{fp}) to be 0.0015 eV below the valence-band maximum. We take the conduction-band discontinuity between the GaAs and the $\text{Al}_x\text{Ga}_{1-x}\text{As}$ layers to be 0.22 eV. We also assume that the conduction-band energy of the *i*-type $\text{Al}_y\text{Ga}_{1-y}\text{As}$ layer is 0.012 eV higher than that of $\text{Al}_x\text{Ga}_{1-x}\text{As}$ layers. We will choose the widths L_{ip} and L_{in} of the undoped *i*-type $\text{Al}_x\text{Ga}_{1-x}\text{As}$

and i_n -type $\text{Al}_y\text{Ga}_{1-y}\text{As}$ layers in accordance with the requirements of the particular mode of operation.

Figure 1(b) shows the generic energy-band diagram of the heterostructure, when the residual built-in potential $V_d - V_j(t)$ is about 0.02 V. As a result of the transverse-momentum conservation during the tunneling process, resonant tunneling of an electron (hole) is only allowed when the junction voltage is such that

$$E_{fn} - e^2/2C_{n-i} \geq E_{\text{res},e} \geq E_{nc} - e^2/2C_{n-i}$$

$$(E_{fp} + e^2/2C_{p-i} \leq E_{\text{res},h} \leq E_{pv} + e^2/2C_{p-i}).$$

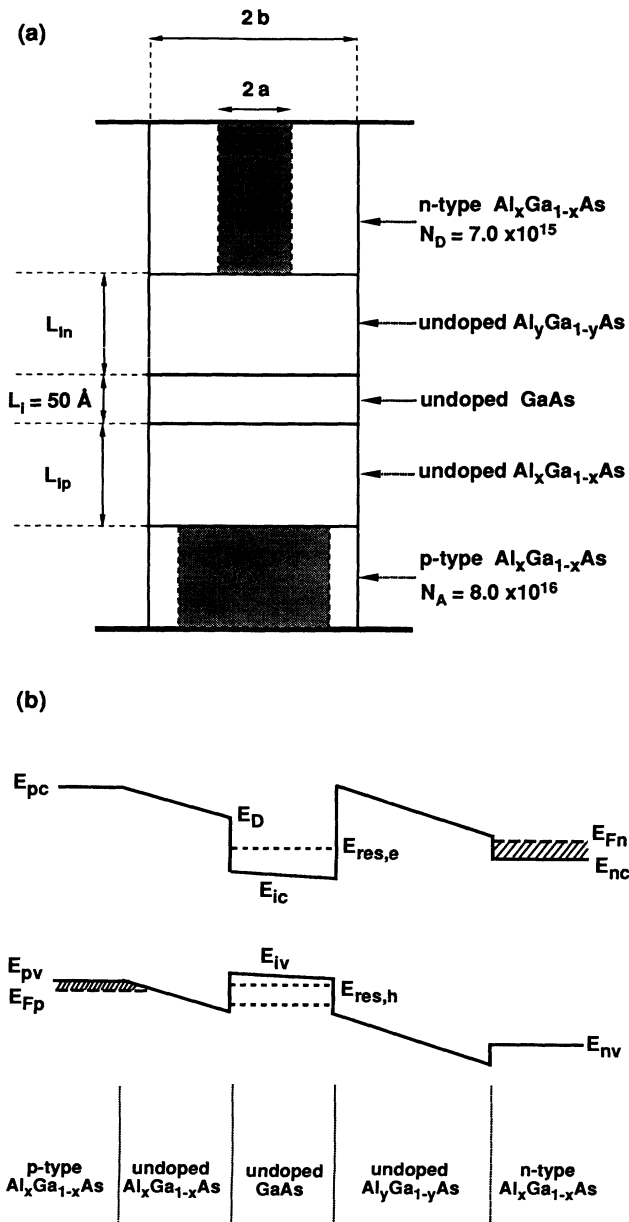


FIG. 1. (a) The detailed structure of the p - i - i - i - n $\text{Al}_x\text{Ga}_{1-x}\text{As}$ -GaAs microjunction. The unshaded regions are depleted. (b) Diagram of the energy band when the residual built-in potential is approximately 0.02 V.

Here, E_{nc} (E_{pv}) denotes the conduction (valence) -band minimum (maximum) energy of the n (p) layer. $E_{\text{res},e}$ ($E_{\text{res},h}$) is the energy of the electron (hole) resonant subband of the i -type quantum well and C_{n-i} (C_{p-i}) is the capacitance of the n - i - i (p - i - i) structure.

In Sec. II, we analyze the dynamics of the heterojunction of Fig. 1(a) under constant-current operation. We show that single-electron charging effects in this case regulate the electron resonant-tunneling events from the n layer into the i layer and result in nonstochastic sawtooth oscillations of the junction voltage. It is assumed here that L_{ip} is much smaller than L_{in} and a relatively high heavy-hole concentration is maintained in the i -type GaAs layer. Provided that the radiative recombination is fast compared to the single-electron charging rate I/e , the junction in this regime will generate a regulated photon stream.^{7,8}

The constant-voltage operation is considered in Sec. III. In this case, L_{ip} and L_{in} are comparable and large enough that the electron and hole tunneling are small compared to the radiative recombination rate. We show here that it is possible to obtain a strict ordering of the basic physical processes: Initially, the i -type GaAs quantum well is empty and the junction voltage is set such that only resonant electron tunneling is allowed. Tunneling of a single electron lifts the energy of the well by e^2/C_{n-i} , which in turn blocks a second electron tunneling event and opens the channel for hole tunneling. After a single-hole tunneling takes place, radiative recombination and further electron tunneling becomes possible. We will show that the radiative recombination and resonant-tunneling events are correlated in this case, even though individual resonant-tunneling events are randomized by the fast circuit recovery time (i.e., constant-voltage operation). We discuss the analogy between this system and the single-atom resonance fluorescence. Finally, in Sec. IV, we discuss the limitations and possible extensions into devices with smaller size.

II. REGULATION OF RESONANT TUNNELING UNDER CONSTANT CURRENT OPERATION

In this section, we show that the resonant-tunneling events in the p - i - i - i - n $\text{Al}_x\text{Ga}_{1-x}\text{As}$ -GaAs heterostructure of Fig. 1(a) can be regulated by the Coulomb interactions. In order to simplify the dynamics, we choose a very short i_p layer width ($L_{ip} = 20 \text{ \AA}$). In this limit, the hole tunneling rate into and out of the i -type GaAs quantum well is much larger than that of electrons and a (high) constant-hole density is maintained inside this undoped layer (modulation doping).¹¹ Therefore, unlike the n - i - i - i - n structures previously studied,^{5,6} resonant tunneling of an electron in the present case will be followed by radiative recombination.

The scheme proposed in this section can be considered analogous to a constant-current-driven double-barrier (thick-thin) tunneling heterostructure: The resonant tunneling through the thin barrier is replaced by radiative recombination in the present case. The (fast) tunneling across the thin barrier (i.e., radiative recombination) is allowed only after a (slow) tunneling event across the thick

barrier takes place. By tunneling directly into the lowest conduction subband, we can enhance the rate at which a free-electron-hole pair decays into the lowest-energy excitonic state, which subsequently (radiatively) recombines in a very short time scale.

The physical principle underlying the Coulomb-blockade effects in the present scheme is similar to that of Ref. 7: If the capacitance of the depletion layer is such that the voltage drop across the junction following a single-electron resonant-tunneling event (e/C_{n-i}) exceeds several kT/e , then a second tunneling event is blocked until the junction voltage is restored to its initial value. Under constant-current operation, the junction voltage increases monotonically (linear or quadratic, depending on the system parameters) in time, with a characteristic time scale e/I , where I is the magnitude of the average current driving the junction. As a result, the resonant-tunneling events occur regularly at time intervals e/I and the junction voltage exhibits nonstochastic oscillations. Provided that the electrons tunneled into the i -type GaAs layer recombine fast compared to e/I , the junction will generate a regulated single-photon stream.

The length of the n (and/or p)-type $\text{Al}_x\text{Ga}_{1-x}\text{As}$ layer [Fig. 1(a)] is important in the constant-current operation, as this section of the structure provides the required high-series impedance R_s . For R_s that exceeds $30\text{ M}\Omega$, this length should be more than $10\text{ }\mu\text{m}$. The width L_{in} of the i_n layer determines the capacitance C_{n-i} and the peak electron tunneling rate into the resonant subband. Here, we choose it to be 410 \AA .

The Coulomb blockade in a microjunction requires that the single-electron charging energy be large compared to the characteristic energy of the thermal fluctuations ($e^2/C \gg kT$) and that the magnitude of the source resistance R_s exceed the resistance quantum $R_Q = 0.5h/e^2$ and $e/[\langle I(t) \rangle C]$. An additional fundamental requirement in the case of resonant tunneling is $e^2/C \gg \hbar(\Gamma + \Delta\omega)$, where Γ and $\Delta\omega$ denote the homogeneous and inhomogeneous widths of the lowest resonant subband, respectively. When these three conditions are satisfied, the resonant-tunneling events into the lowest subband will be regulated. If the tunneling occurs into a high-lying subband, an additional requirement for the regulation of the tunneling events is to have a subband spacing that exceeds the single-electron charging energy.

The tunneling rate for an electron originally in the n layer into the i layer is given by¹¹

$$R_t = \frac{kTm_e^*}{2\pi^2\hbar^3} A_{\text{eff}} \times \int_{E_c}^{\infty} T(E_z) \ln \left[1 + \exp \left(\frac{E_{fn} - E_z}{kT} \right) \right] dE_z, \quad (1)$$

where

$$T(E_z) = \frac{k_2^2 + \kappa_2^2}{k_1^2 + \kappa_1^2} \frac{4k_1^2\kappa_1^2}{|\Delta k|^2} \exp \left[\int_0^{L_{in}} \kappa_1(z) dz \right], \quad (2a)$$

$$\Delta k = (k_2\kappa_2 - k_2\kappa_1) \cos(k_2L_i) - (k_2^2 + \kappa_1\kappa_2) \sin(k_2L_i), \quad (2b)$$

$$k_1 = \frac{\sqrt{2m_e^*(E_z - E_{nc})}}{\hbar}, \quad (2c)$$

$$\kappa_1(z) = \frac{\sqrt{2m_e^*}}{\hbar} \left[E_{c-ex} + E_{nc} - E_z + (E_D - E_{nc} + e^2/2C_{n-i}) \frac{z - z_n}{L_{in}} \right]^{1/2}, \quad (2d)$$

$$k_2 = \frac{\sqrt{2m_e^*(E_z - E_{ic} - e^2/2C_{n-i})}}{\hbar}, \quad (2e)$$

$$\kappa_2(z) = \frac{\sqrt{2m_e^*}}{\hbar} \left[E_{cp} - E_z + E_{ic} + e^2/2C_{n-i} - eV_{j2}(t) + [eV_{j2}(t) + e^2/2C_{p-i}] \frac{z - z_{ip}}{L_{ip}} \right]^{1/2}. \quad (2f)$$

Here m_e^* denotes the effective mass of a conduction-band electron, which is taken to be independent of the Al concentration. E_{ic} and E_{pc} refer to the conduction-band (minimum) energy in the i and p layers, respectively. $E_D - E_{ic}$ ($-E_{c-ex}$) gives the conduction-band discontinuity between the $\text{Al}_x\text{Ga}_{1-x}\text{As}$ and GaAs ($\text{Al}_y\text{Ga}_{1-y}\text{As}$) materials. E_z is the energy corresponding to the longitudinal (z) motion of a plane-wave electron (with longitudinal momentum k_z) incident on the n - i_n layer boundary and $V_{j2}(t)$ is the part of the junction voltage that is spanned by the i_p layer. The expressions given in Eqs. (2d) and (2f) are valid only when the width of the n (p) depletion layer is small compared to L_{in} (L_{ip}). In obtaining Eq. (1), the WKB approximation is used and it is assumed that (1) the device is operated in the strong tunneling regime

$$\left[\int_0^{L_{in}} \kappa_1(z) dz \gg 1 \right],$$

and (2) the electric field in between the p and n depletion layers is small enough that we can take k_2 to be independent of z . Unless the z dependence is indicated, we take κ_1 and κ_2 to be the space-averaged value of $\kappa_1(z)$ and $\kappa_2(z)$, respectively. Within these approximations, only the conduction-band energy E_{nc} on the n side is a function of the junction voltage $V_j(t)$ and is given by

$$E_{nc} = E_D + eV_j(t) - eV_d,$$

where V_d is the built-in potential. Finally, we note that Eq. (1) may be used to calculate the hole-tunneling rate from the p layer into the i -type quantum well.

Equation (2a) predicts that when $\Delta k = 0$, the transmission coefficient $T(E_z)$ will diverge. This resonance condition is given by

$$\tan(k_2 L_i) = \frac{k_2 \kappa_2 - k_2 \kappa_1}{k_2^2 + \kappa_1 \kappa_2} \quad (3)$$

In a quantum well with nonzero homogeneous broadening, the transmission coefficient given by Eq. (2a) is no longer correct for incident electron energies that satisfy Eq. (3). We assume that to correctly describe the dynamics at or near resonance at very low temperatures, one should modify Δk by

$$\Delta k - i\Gamma m_e^* / \hbar, \quad (4)$$

where Γ is the homogeneous width of the resonance resulting from the dephasing and the inelastic decay mechanisms as well as the tunneling process itself. The effect of inhomogeneous broadening can be incorporated by convolving the transmission coefficient of Eq. (2a) by a Gaussian distribution of resonant subband energies. In this work, however, we will assume that the inhomogeneous width of the subband is negligible compared to its homogeneous width.

We will assume that the decay rate Γ is dominated by

the energy-relaxation rate of the subband into a (hot) excitonic state by emission of a phonon. We will take this rate to be $5 \times 10^{10} \text{ s}^{-1}$, corresponding to a decay time of 20 psec. We believe that this is a reasonable assumption since total dephasing times well above 20 psec have been demonstrated experimentally for high-purity GaAs samples.¹² The rate at which a free electron in the lowest subband recombines with a hole is determined by the (slow) thermalization rate of a high-kinetic-energy exciton into a $k_{\text{exc}} \leq k_{\text{photon}}$ heavy-hole exciton, as this is the only excitonic state that is allowed to recombine radiatively.¹³ The excitonic recombination times (for excitons with $k_{\text{exc}} \leq k_{\text{photon}}$) are demonstrated to be as low as 10 psec (Ref. 14) and therefore do not impose any limitation on the effective recombination rate. We assume that the thermalization rate is such that the total *effective* recombination time in this sequential process at $T=0.3 \text{ K}$ is 150 psec. The direct recombination time of a free electron with a free hole is longer than 1 nsec and is, in general, slower than this sequential process.¹³

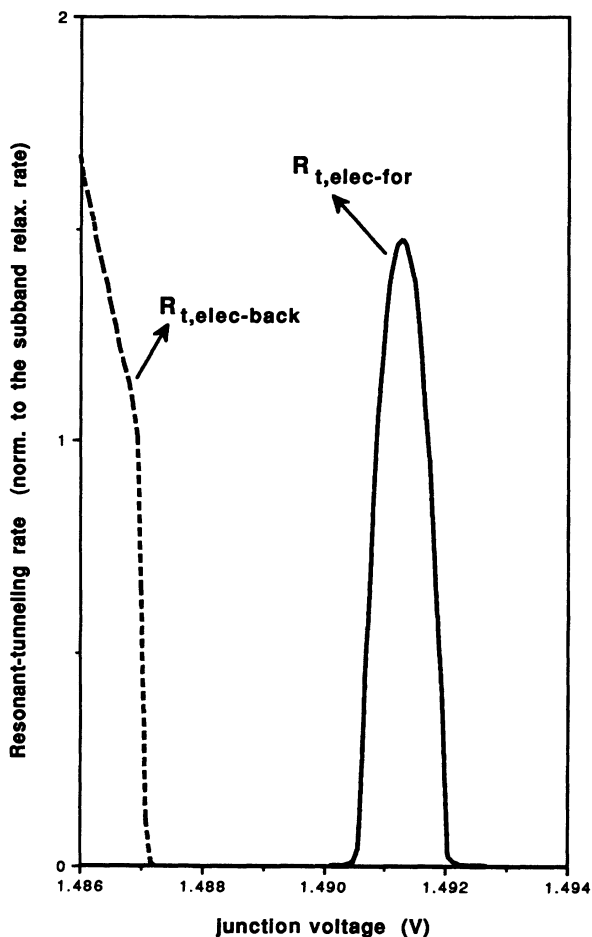


FIG. 2. Resonant-tunneling rates into ($R_{t,\text{elec-for}}$) and out of ($R_{t,\text{elec-back}}$) the *i*-type GaAs quantum well as a function of the junction voltage. Both rates are normalized to the energy-relaxation rate $\Gamma_{\text{relax}} = 5.0 \times 10^{10} \text{ s}^{-1}$ of the resonant subband.

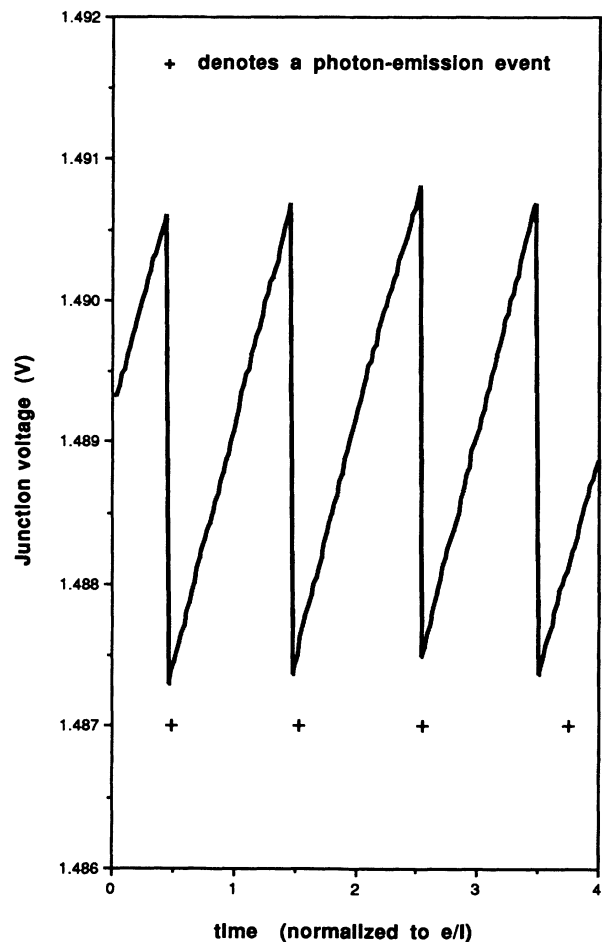


FIG. 3. The junction voltage as a function of time for a junction with a source resistance $R_s = 300 \text{ M}\Omega$ and a driving ideal-voltage source $V_{in} = 1.53 \text{ V}$ ($e/\langle I \rangle = 1.5 \text{ ns}$) at $T = 0.3 \text{ K}$. The pluses in the figure denote the accompanying radiative recombination events.

By investigating Eq. (3), we see that when $k_2 \gg \kappa_1 > \kappa_2$, the energy of the lowest allowed subband for the conduction-band electron inside the i -type quantum well is approximately given by

$$E_{ic} + (\hbar\pi/L_i)^2/2m_e^* .$$

For a well width of $L_i = 50 \text{ \AA}$, this is approximately $E_{ic} + 0.2 \text{ eV}$. At $T = 0.3 \text{ K}$, with a source resistance of $R_s = 300 \text{ M}\Omega$ and a driving ideal voltage source of 1.53 V , the operating junction voltage and current are roughly 1.49 V and 0.1 nA , respectively. For this junction-voltage level, the depletion-layer capacitance is approximately given by $5 \times 10^{-17} \text{ F}$.

Figure 2 shows the resonant-tunneling rates into ($R_{t,\text{elec-for}}$) and out of ($R_{t,\text{elec-back}}$) the quantum well as a function of the junction voltage for the given junction parameters. We see that the tunneling rate into the well increases exponentially with the increasing junction voltage for $V_j < 1.4905 \text{ V}$, flattens out at a value of $6 \times 10^{10} \text{ s}^{-1}$ when $1.4905 < V_j < 1.492 \text{ V}$, and decreases exponentially

for $V_j > 1.492 \text{ V}$. The width of the resonant-tunneling window is roughly given by $E_{fn} - E_c$ in this case, as the width Γ of the resonant level is much smaller. The back-tunneling rate $R_{t,\text{elec-back}}$ for $V_j < 1.487$ is a rather slow function of the junction voltage and the functional dependence is determined by the transmission coefficient. For $V_j \geq 1.487 \text{ V}$, however, $R_{t,\text{elec-back}}$ decreases exponentially, due to the Pauli exclusion principle: The energy of the quantum-well electron in this junction-voltage range is smaller than $E_{fn} + e^2/2C$ and, therefore, the number of available final states is greatly reduced.

We have chosen the i_n -type $\text{Al}_y\text{Ga}_{1-y}\text{As}$ barrier width such that the peak resonant-tunneling rate into the well is not much larger than the energy-relaxation rate of the quantum-well subband. By doing so, we suppress the back-tunneling probability of an electron that has tunneled into the well. If this were not the case, the electron would tunnel back and forth many times and create high-frequency junction-voltage noise.

The simulation of the junction dynamics that we carried out uses the Monte Carlo method and is very similar

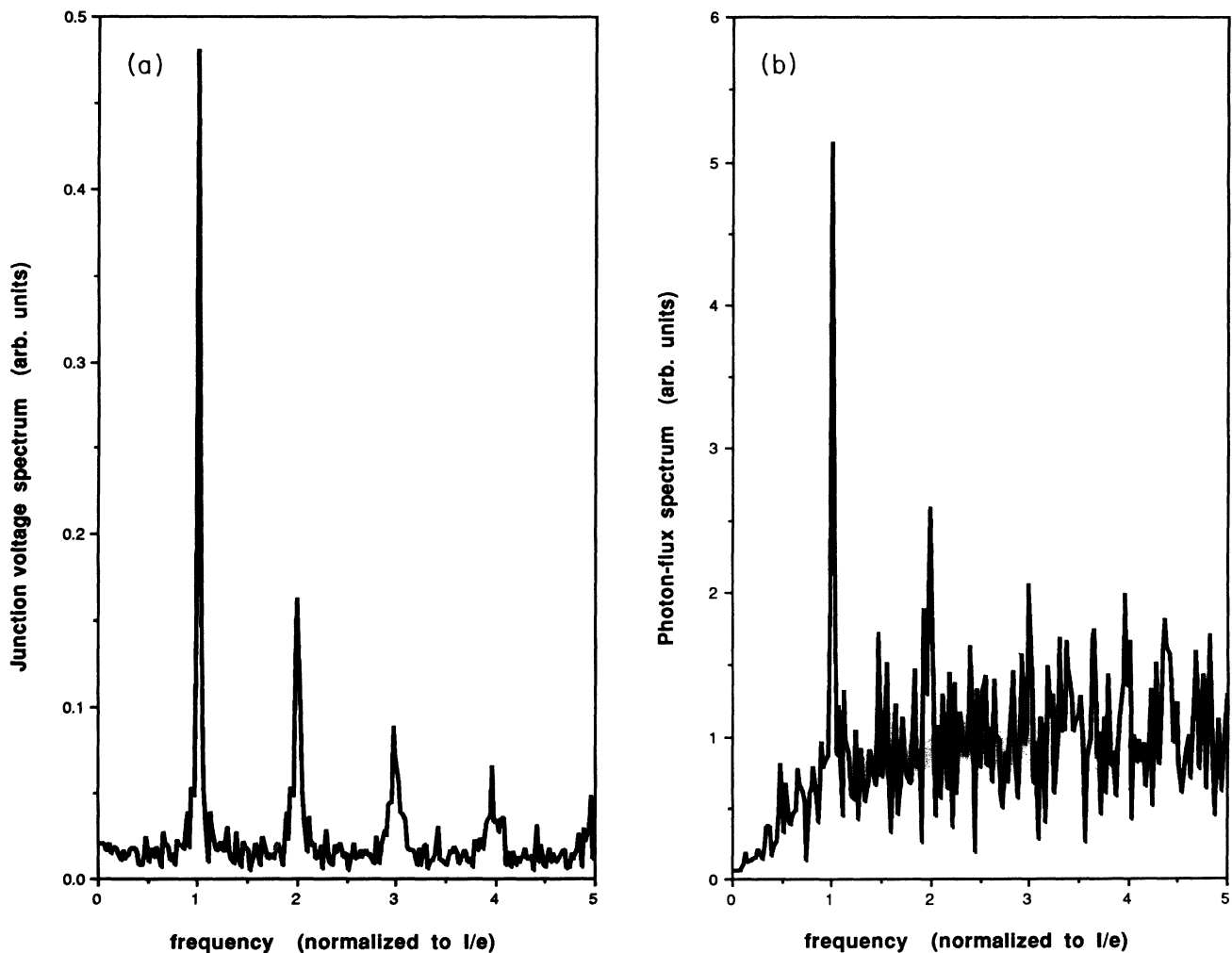


FIG. 4. The spectrum of (a) the junction voltage and (b) the photon stream, for $R_s = 300 \text{ M}\Omega$, $T = 0.3 \text{ K}$, and $V_{in} = 1.53 \text{ V}$. The autocorrelation function of the photon stream is shown in (c).

to the one used in Ref. 7. We therefore skip the details and refer the reader to that paper. As we have mentioned earlier, we assume in the simulation that the hole density in the *i*-type GaAs layer is constant due to a balance of (fast) hole-tunneling rates $R_{t,\text{hole-for}}$ and $R_{t,\text{hole-back}}$. Immediately following an electron-tunneling event, an additional hole tunnels into the well so as to keep the net charge density constant. Figure 3 shows the simulation result of the junction voltage as a function of time, together with the accompanying photon-emission events. The regularity of the junction-voltage oscillations is evident. The photon emission occurs in an average waiting time of about $0.1 \times e / \langle I(t) \rangle \approx 150$ psec.

Figure 4(a) shows the spectrum of the junction voltage, where up to the fourth harmonic of $\langle I(t) \rangle / e$ can be clearly observed above the background noise. The number of observed harmonics can be regarded as a measure of how well the tunneling events are regulated. In the case of junction voltage, the determining factor is the ratio of the average waiting time for tunneling (τ_{tunn}) to the single-electron charging time [$e / \langle I(t) \rangle$]. In the limit of very large peak tunneling rates

$$[R_{t,\text{peak}} \gg \langle I(t) \rangle / e]$$

and under constant-current operation, the average waiting time for the *first* tunneling event would approach the average waiting time $\tau_{te} = kT / e^2 / C \langle I(t) \rangle / e$ obtained in Ref. 7. In this limit, τ_{tunn} will be determined by the larger of the τ_{te} and the energy-relaxation time of the resonant subband. In the limit of low peak tunneling rates, the waiting time is determined by the peak resonant-tunneling rate itself. The case of Fig. 3 is somewhere in between these limits and the (observed) average waiting time is about 50 psec. Figure 4(b) shows the spectrum of the generated photon flux: Only the first and second harmonics are above the background-noise level in this case, since the presence of an additional stochastic process (thermalization followed by radiative recombination) introduces additional jitter.

Figure 4(c) shows the autocorrelation function $A(t)$ of the generated photons: The fact that $A(t)$ is far below 1 for $t < e / \langle I(t) \rangle$ is an indication that the photon stream is antibunched and strongly sub-Poissonian. The peaks at the integer multiples of $e / \langle I(t) \rangle$ indicate that additional information about the photon-emission times is available: in the case of a photon stream generated by a constant-current-driven microjunction, we know not only the total number of photons emitted in a certain time interval, but also the precise emission time for each photon.

The dependence of the junction-voltage oscillations on the magnitude of the source resistance, the shunt capacitance, and temperature was analyzed in detail in Ref. 7. As the two systems are qualitatively similar in terms of their dependence on these parameters, we chose not to reproduce those results here. The principal result of that analysis is that $e^2 / (C_{n-i} + C_s) \gg kT$ and

$$R_s > e / [\langle I(t) \rangle C_{\text{dep}}]$$

are required for the regulation of junction-voltage oscillations. It was also shown in Ref. 7 that the average I - V characteristics of a constant-current-driven *p-p-i-n* junction is modified due to the single-electron charging effects. The same conclusion applies to the heterostructure of Fig. 1(a); however, obtaining a general analytical expression is significantly harder.

III. CONSTANT-VOLTAGE OPERATION

The difficulty in manufacturing microstructures with high source impedances at the junction-voltage oscillation frequency I/e stimulated research on the demonstration of the Coulomb-blockade effects under constant-voltage operation. It has been shown both theoretically and experimentally that correlations between successive resonant-tunneling events in a constant-voltage-driven multijunction system result in conductance oscillations and a Coulomb-staircase structure in the average I - V characteristics.³⁻⁶ In this section, we show that single-electron (hole) charging effects will result in correlations between the resonant-tunneling and photon-emission events in constant-voltage-driven *p-i-i-i-n* semiconductor heterostructures. As a result of these correlations the

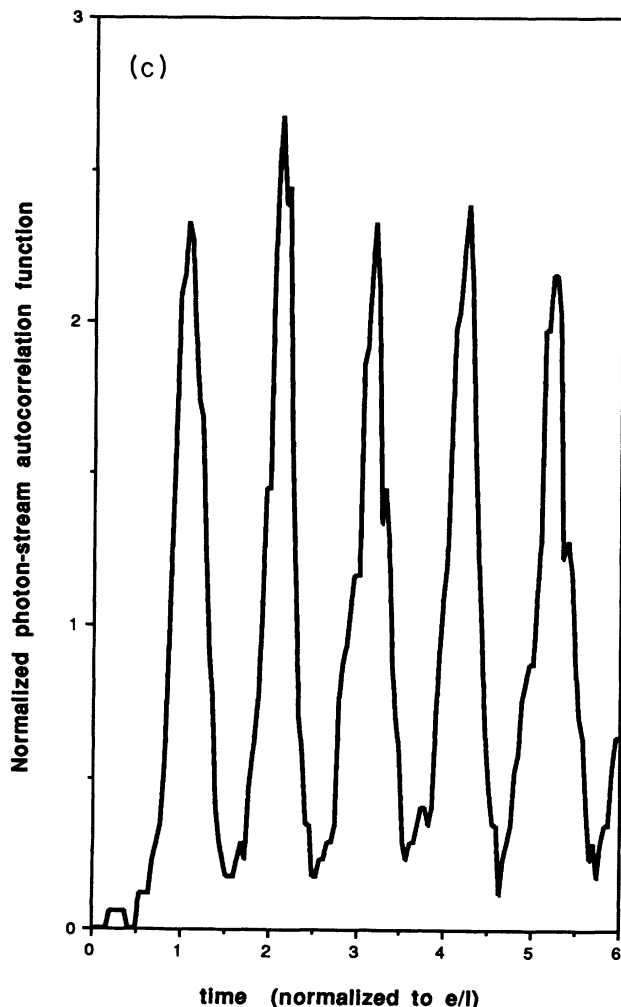


FIG. 4. (Continued).

generated photons are antibunched and sub-Poissonian.

When the width L_{ip} of the i_p layer is increased such that the capacitance of the p - i_p - i section of the heterostructure becomes comparable to that of the n - i_n - i section, the hole-tunneling rate $R_{t,\text{hole}}$ (into the well) will become comparable to that of an electron. We use Eq. (1) to calculate $R_{t,\text{hole}}$ for a heavy hole, after replacing the conduction-band parameters with those of the valence band. We assume that the conduction- and valence-band discontinuities have a ratio of 3:2 for all values of Al concentrations of interest. Increasing the band gap of the $\text{Al}_y\text{Ga}_{1-y}\text{As}$ layer increases the relative energy of the hole subband with respect to E_{fp} (i.e., $|E_{\text{res},h} - E_{fp}|$) and decrease $|E_{\text{res},e} - E_{fn}|$, provided that $E_D + E_{c-\text{ex}} > E_{pc}$. This feature not only allows us to move the electron and hole subbands as desired, but also reduces the $R_{t,\text{elec}}$ ($=R_{t,\text{elec-for}}$) by introducing an additional barrier for electron tunneling. The circuit recovery time $R_s C_{\text{tot}}$ is much shorter than the other time scales and in practice a constant voltage is maintained across the junction at all times. As a result of this, back-tunneling of both elec-

trons and holes is virtually eliminated, irrespective of the peak tunneling rates.

For the ideal operation, the electron and hole subband energies should be chosen such that the peak tunneling rate into the hole subband is obtained at a junction-voltage value that is e/C_{n-i} larger than that required for the peak tunneling rate into the electron subband. The Fermi energy as measured from the conduction- or valence-band minima should also be small compared to e^2/C_{n-i} and e^2/C_{p-i} : This will guarantee that only electron or hole tunneling (not both) will be important at any given junction voltage. One then sets the junction voltage to the value that results in the highest-electron resonant-tunneling rate. During the waiting time for electron tunneling ($\tau_{e-\text{wait}} = R_{t,\text{elec-peak}}^{-1}$) the hole-tunneling probability is negligible. After an electron tunnels, the energy of the well is increased by e^2/C_{n-i} and further electron tunneling is strictly blocked, even though the junction voltage quickly recovers to its original value. Now that an electron is present in the well, the junction voltage required for peak hole tunneling is decreased by

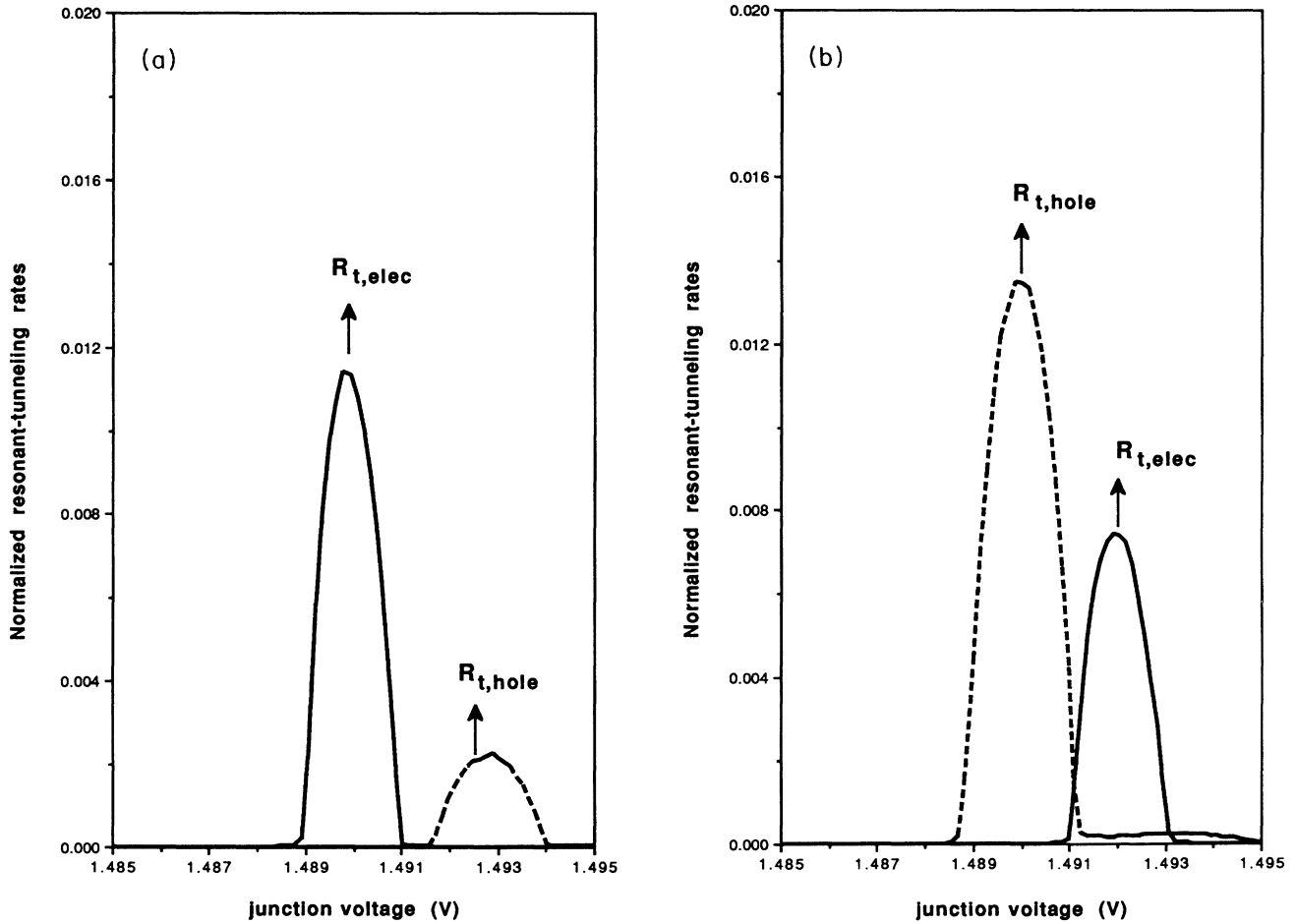


FIG. 5. The electron ($R_{t,\text{elec}}$) and hole ($R_{t,\text{hole}}$) resonant-tunneling rate into the quantum well as a function of the junction voltage, when (a) $n_{\text{elec}} = n_{\text{hole}}$, and (b) $n_{\text{elec}} = n_{\text{hole}} + 1$. Here, n_{elec} and n_{hole} denote the total number of electrons and holes in the quantum well, respectively. All rates are normalized to Γ_{relax} .

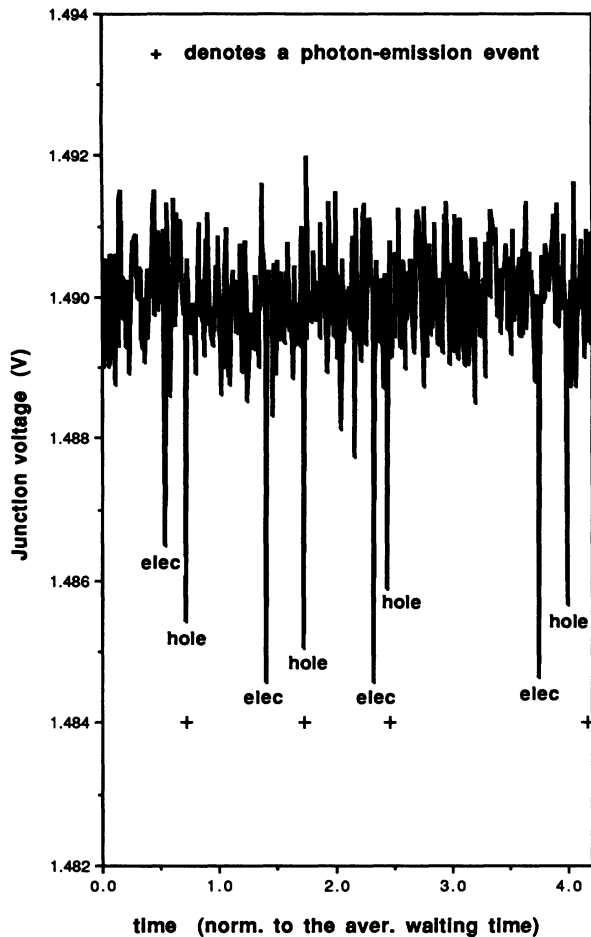


FIG. 6. Junction voltage as a function of time for $R_s = 3 \text{ M}\Omega$, $T = 0.3 \text{ K}$, and $V_{in} = 1.490 \text{ V}$. The voltage spikes are associated with electron- and hole-tunneling events. The pluses denote the accompanying radiative recombination events.

about e^2/C_{n-i} and, therefore, hole-tunneling probability is resonantly enhanced. After the single-hole tunneling takes place, the junction is back to its original state, as the electron and the hole in the well neutralize each other and no longer affect the junction dynamics. This sequential nature of the electron and the hole-tunneling events result in “antibunching”¹⁰ of tunneling events; the tunneling events are no longer Poissonian and there is a “dead” period after each electron (hole) tunneling, during which the junction waits for a hole (electron) tunneling. The radiative recombination inside the i -type GaAs layer can only occur if there is at least one electron and one hole. Provided that the recombination rate is fast compared to the peak electron- or hole-tunneling rates, the antibunching of the tunneling events is transformed into an antibunched photon field. The degree of antibunching is well measured by the intensity autocorrelation function $A(t)$ of the photon stream.¹⁰

In the numerical simulation, we assume that $L_{ip} = 620 \text{ \AA}$ and $L_{in} = 580 \text{ \AA}$. With the chosen source resistance of

$3 \text{ M}\Omega$, the circuit recovery time $R_s C_{tot}$ is shorter than all the other relevant time scales. Figure 5(a) shows the electron- and hole-tunneling rates as a function of the junction voltage when the number of electrons (n_{elec}) in the well is equal to that of holes (n_{hole}): The peaks in the tunneling rates are separated by about e/C_{n-i} . After an electron tunneling takes place ($n_{elec} = n_{hole} + 1$), the tunneling rates are shifted in opposite directions, as shown in Fig. 5(b). By choosing $V_{in} = 1.490 \text{ V}$, we can resonantly enhance either the electron ($n_{elec} = n_{hole}$) or hole ($n_{elec} = n_{hole} + 1$) tunneling, while suppressing the other.

Figure 6 shows the result of the simulation of junction voltage and photon emission at $T = 0.3 \text{ K}$: The principal result here is that electron- and hole-tunneling events are sequential and are strongly correlated with the photon-emission events. Each hole- and electron-tunneling event creates a voltage spike. Although the generated photon stream is not regulated (due to the stochastic nature of the individual tunneling events once the blockade is lifted), it is antibunched due to the average waiting time required for another sequence of tunneling events to occur. Figure 7(a) shows the autocorrelation of the photon stream generated by a sample junction. The value of the autocorrelation is clearly below unity for approximately

$$t \leq \tau_{wait} \approx R_{t,elec\text{-peak}}^{-1} + R_{t,hole\text{-peak}}^{-1},$$

indicating that photon-emission events are anticorrelated. Figure 7(b) shows the corresponding photon-stream spectrum, where the normalization is with respect to a Poissonian photon stream with the same number of average photons. For frequencies below τ_{wait}^{-1} , the spectrum is below the shot-noise limit, indicating the sub-Poissonian nature of the generated photon stream.

It has been demonstrated by Kimbel, Dagenais, and Mandel¹⁰ that resonance fluorescence from a single two-level atom is antibunched: Following each photon emission by an excited-state atom, there is a dead period in fluorescence. This is due to the simple fact that the atom is now in the ground state and it has to be repumped into an excited state before it is allowed to fluoresce once again. We believe that our scheme is analogous to a two-state atom, where excited-state fluorescence is replaced by hole tunneling, and repumping is replaced by electron tunneling. The antibunched fluorescence in our case is a by-product of the antibunched tunneling events and has no effect on the junction dynamics.

As can be deduced from Fig. 6, the “spikes” in the junction voltage caused by electron-hole correlations carry information about the associated photon-emission events. This information can, in principle, be extracted by simultaneous measurement of the photon number and the junction voltage.⁵

IV. DISCUSSION

A limitation of the heterostructure of Fig. 1(a), especially under constant-current operation, is that there is a time delay between the regulated single-electron tunneling events into the i -type GaAs quantum-well subband and the photon-emission events from the excitonic recombination. This time delay, as mentioned before, is

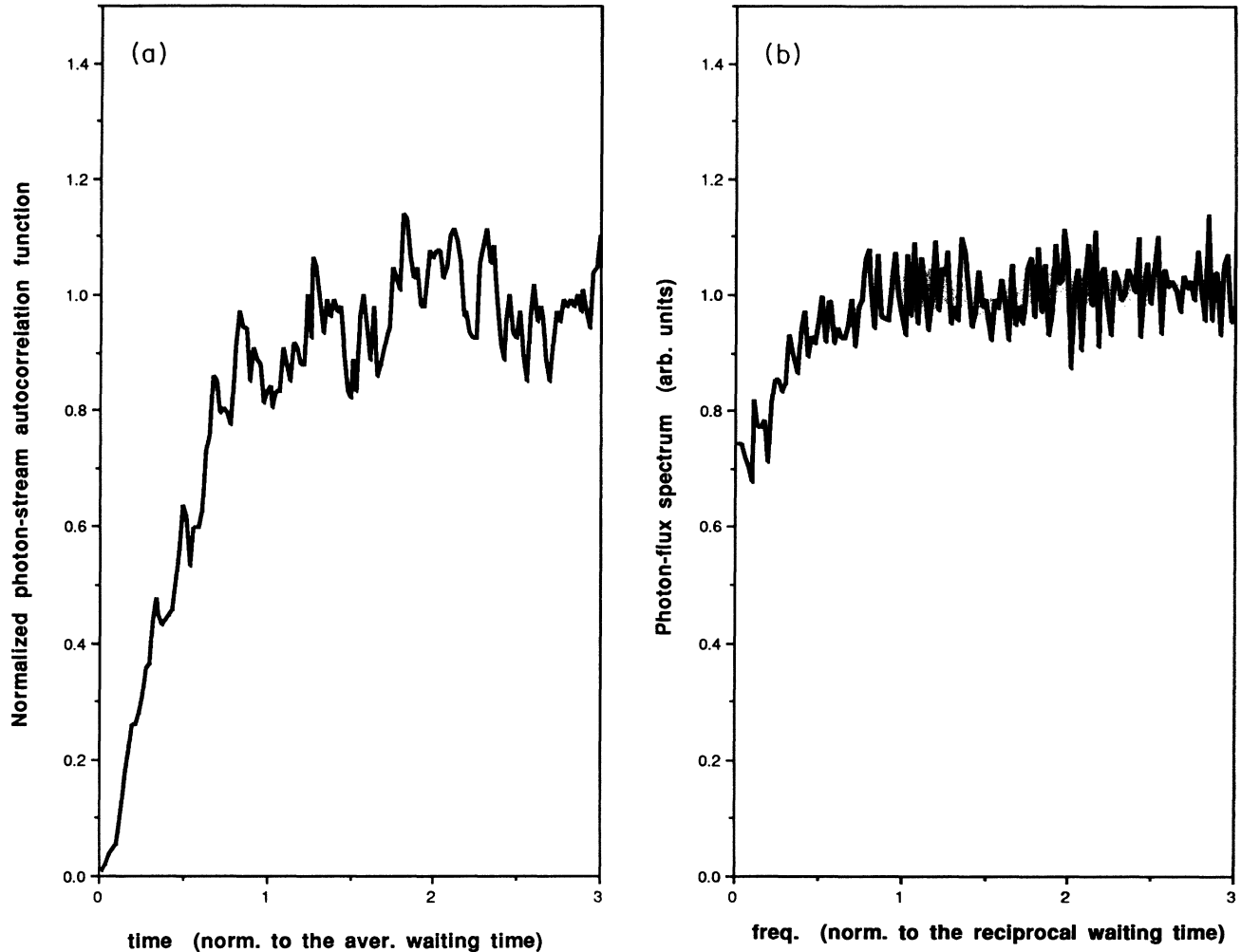


FIG. 7. (a) The autocorrelation function of the photon stream generated by the junction when $R_s = 3 \text{ M}\Omega$, $T = 0.3 \text{ K}$, and $V_{in} = 1.490 \text{ V}$, and (b) the associated spectrum. The spectrum is normalized to that of a Poissonian photon stream.

primarily due to the time it takes for a free electron to relax down to the lowest-energy excitonic state. Radiative recombination from an excitonic state is enhanced by a factor proportional to the ratio of the coherence area of the quantum-well exciton to πa_B^2 (where a_B is the Bohr radius of the exciton), due to the correlation between the electron and hole sites.^{14,16} The direct tunneling rate into an excitonic state is smaller than that of a subband by at least the same ratio, and is therefore negligible in the case of quantum wells. As the lateral dimensions become on the order of the Bohr radius of an exciton, however ($a \leq a_{\text{Bohr-exc}} \approx 100 \text{ \AA}$), the distinction between a free-electron-hole state and an excitonic state disappears.¹¹ In this quantum-box limit, one can simultaneously convert the resonant-tunneling events into photon-emission events by utilizing the fast, direct recombination rates of the electronic states into which tunneling occurs.

The generation of single-photon states of a given radiation-field model from the device proposed here will only occur if the spontaneous recombination is directed by a microcavity structure,⁹ in which the heterostructure of Fig. 1 is embedded. Such a microcavity structure may also be used to enhance the direct recombination rate of

the free-electron-hole pair. In principle, this is an alternative method to achieve fast recombination rates, required for high average current [$\langle I(t) \rangle$] operation. Finally, the tunneling events in this work are assumed to be instantaneous. Provided that the tunneling time¹⁷ is short compared to the energy-relaxation time of 20 psec and the average waiting time for tunneling, this assumption is well justified.

The principal result of this paper is the demonstration of the possibility of single-electron-to-single-photon conversion using the Coulomb blockade of resonant tunneling. Under constant-current operation, the generated photon field is a single-photon stream, which may be considered a "strongly antibunched photon-number state." The antibunching property exists under constant-voltage operation as well. To the best of our knowledge, this is the first prediction of nonclassical photon generation by constant-voltage-driven semiconductor heterojunctions. We believe that this result will prove to be useful in optoelectronic communications technology in the future, as it provides a link between the emerging fields of single electronics¹ and photonics. The key concept applies ideally for quantum devices with lower dimensions.

- ¹D. V. Averin and K. K. Likharev, *J. Low Temp Phys.* **62**, 345 (1986).
- ²E. Ben-Jacob, Y. Gefen, K. Mullen, and Z. Schuss, *Phys. Rev. B* **37**, 7400 (1988).
- ³T. A. Fulton and G. J. Dolan, *Phys. Rev. Lett.* **59**, 109 (1987); J. B. Barner and S. T. Ruggiero, *ibid.* **59**, 807 (1987); L. S. Kuz'min and K. K. Likharev, *Pis'ma Zh. Eksp. Teor. Fiz.* **45**, 389 (1987) [*JETP Lett.* **45**, 495 (1987)].
- ⁴C. W. J. Beenakker, *Phys. Rev. B* **44**, 1646 (1991); C. W. J. Beenakker and H. van Houten, *Solid State Phys.* **44**, 1 (1991); H. van Houten, C. W. J. Beenakker, and A. A. M. Staring, in *Single Charge Tunneling*, edited by H. Grabert and M. H. Devoret (Plenum, New York, 1991).
- ⁵D. V. Averin, A. N. Korotkov, and K. K. Likharev, *Phys. Rev. B* **44**, 6199 (1991); A. Groshev, *ibid.* **42**, 5895 (1990); U. Meirav, M. A. Kastner, and S. J. Wind, *Phys. Rev. Lett.* **65**, 771 (1990).
- ⁶P. L. McEuen, E. B. Foxman, U. Meirav, M. A. Kastner, Y. Meir, N. S. Wingreen, and S. J. Wind, *Phys. Rev. Lett.* **66**, 1926 (1991); P. Gueret, N. Blanc, R. Germann, and H. Rothuizen, *ibid.* **68**, 1896 (1992).
- ⁷A. Imamoglu, Y. Yamamoto, and P. Solomon, *Phys. Rev. B* **46**, 9555 (1992).
- ⁸Y. Yamamoto and S. Tarucha, *Jpn. J. Appl. Phys.* **31**, L1198 (1992).
- ⁹G. Bjork, S. Machida, Y. Yamamoto, and K. Igeta, *Phys. Rev. A* **44**, 669 (1991).
- ¹⁰H. J. Kimble, M. Dagenais, and L. Mandel, *Phys. Rev. A* **18**, 201 (1978).
- ¹¹C. Weisbuch and B. Vinter, *Quantum Semiconductor Structures* (Academic, San Diego, 1991).
- ¹²L. Pfeiffer, K. W. West, H. L. Stormer, and K. W. Baldwin, *Appl. Phys. Lett.* **55**, 1888 (1989).
- ¹³T. C. Damen, J. Shah, D. Y. Oberli, D. S. Chemla, J. E. Cunningham, and J. M. Kuo, *Phys. Rev. B* **42**, 7434 (1990).
- ¹⁴B. Deveaud, F. Clerot, N. Roy, K. Satzke, B. Sermage, and D. S. Katzer, *Phys. Rev. Lett.* **67**, 2355 (1991).
- ¹⁵W. H. Richardson and Y. Yamamoto, *Phys. Rev. Lett.* **66**, 1963 (1991).
- ¹⁶E. Hanamura, *Phys. Rev. B* **38**, 1228 (1988); L. C. Andreani, F. Tassone, and F. Bassani, *Solid State Commun.* **77**, 641 (1990).
- ¹⁷M. Buttiker and R. Landauer, *Phys. Rev. Lett.* **49**, 1739 (1982).

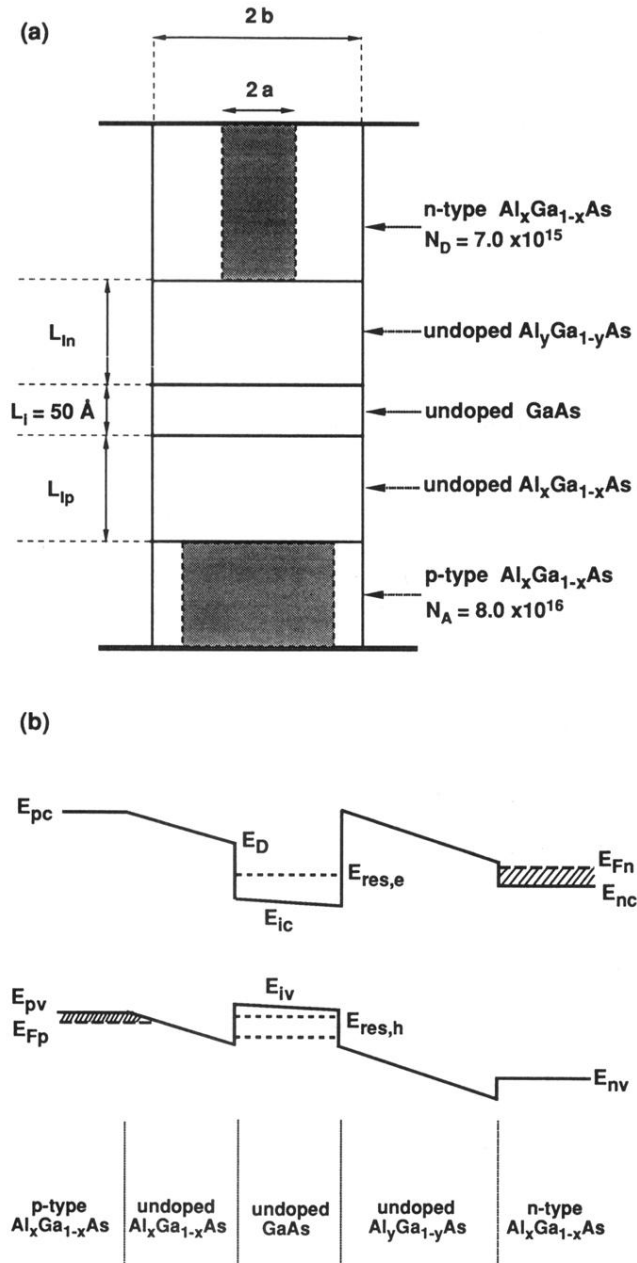


FIG. 1. (a) The detailed structure of the $p-i-i-i-n$ $\text{Al}_x\text{Ga}_{1-x}\text{As}$ -GaAs microjunction. The unshaded regions are depleted. (b) Diagram of the energy band when the residual built-in potential is approximately 0.02 V.